

# Milliarcsecond angular resolution of reddened stellar sources in the vicinity of the Galactic Center <sup>★</sup>

A. Richichi<sup>1</sup>, O. Fors<sup>2,3</sup>, E. Mason<sup>4</sup>, J. Stegmaier<sup>1</sup>, and T. Chandrasekhar<sup>5</sup>

<sup>1</sup> European Southern Observatory, Karl-Schwarzschild-Str. 2, 85748 Garching bei München, Germany e-mail: arichich@eso.org

<sup>2</sup> Departament d'Astronomia i Meteorologia, Universitat de Barcelona, Martí i Franqués 1, 08028 Barcelona, Spain

<sup>3</sup> Observatori Fabra, Camí de l'Observatori s/n, 08035 Barcelona, Spain

<sup>4</sup> European Southern Observatory, Santiago, Chile

<sup>5</sup> Physical Research Laboratory, 380009 Ahmedabad, India

Preprint online version: February 17, 2019

## ABSTRACT

**Aims.** For the first time, the lunar occultation technique has been employed on a very large telescope in the near-IR with the aim of achieving systematically milliarcsecond resolution on stellar sources.

**Methods.** We have demonstrated the burst mode of the ISAAC instrument, using a fast read-out on a small area of the detector to record many tens of seconds of data at a time on fields of few squared arcseconds. We have used the opportunity to record a large number of LO events during a passage of the Moon close to the Galactic Center in March 2006. We have developed and employed for the first time a data pipeline for the treatment of LO data, including the automated estimation of the main data analysis parameters using a wavelet-based method, and the preliminary fitting and plotting of all light curves.

**Results.** We recorded 51 LO events over about four hours. Of these, 30 resulted of sufficient quality to enable a detailed fitting. We detected two binaries with subarcsecond projected separation and three stars with a marginally resolved angular diameter of about 2 milliarcseconds. Two more stars, which are cross-identified with SiO maser, were found to be resolved and in one case we could recover the brightness profile of the extended emission, which is well consistent with an optically thin shell. The remaining unresolved stars were used to characterize the performance of the method.

**Conclusions.** The LO technique at a very large telescope is a powerful and efficient method to achieve angular resolution, sensitivity, and dynamic range that are among the best possible today with any technique. The selection of targets is naturally limited and LOs are fixed-time events, however each observation requires only a few minutes including overheads. As such, LOs are ideally suited to fill small gaps of idle time between standard observations.

**Key words.** Techniques: high angular resolution – Astrometry – Occultations – Binaries – Masers

## 1. Introduction

The method of observing lunar occultations (LO) of background stars to derive their angular diameter, as well as other characteristics such as binarity, has been employed for decades and provides angular resolution at the milliarcsecond (mas) level independently of the diameter of the telescope used. This surpasses the diffraction limit of even the largest single telescopes and rivals the resolution of long-baseline interferometry (LBI) even with baselines of hundreds of meters. Basically, the LO technique relies on the lunar limb as a diffracting edge, rather than on the diameter of the telescope. The diffraction fringes are generated in space, and due to their relatively fast motion over the telescope they must be sampled at rates of order 0.1-1 kHz. Combined together, these factors greatly diminish the adverse effects of atmospheric turbulence, which are the main limit of other high angular resolution techniques. LO also permit not only a model-dependent derivation of source parameters such as the angular diameter and binary parameters, but also a model-independent reconstruction of the brightness profile of the source according to maximum-likelihood, or even a unique reconstruction by light curve inversion in special cases. The time required

for observation (dominated by overheads, since an occultation lasts much less than 1 s) and for data analysis is significantly shorter than for most other high angular resolution methods.

Of course, LO suffer from a number of significant drawbacks, first among them that the sources cannot be chosen at will. The Moon covers only about 10% of the celestial sphere in its apparent orbit. LO are fixed time events, and as such subject to weather and instrumental downtimes. Finally, the lunar limb only provides a 1-D scan of the source, although observations from different sites, or at different epochs, can in principle be combined under favorable circumstances. Due mainly to the chromatic properties of the scattered light background around the Moon and of the diffraction fringes, the near-IR is ideally suited to observe LO. More details on the method, its performance, the data analysis and the results can be found in Richichi (1985, 1996) and Fors (2006). The CHARM2 catalogue alone (Richichi et al. 2005) lists 1815 LO results in the field of high angular resolution.

While the angular resolution of LO is set mainly by the lunar limb rather than by telescope size, this latter parameter obviously has a crucial role in determining the limiting sensitivity. Richichi (1997) studied the performance of LO under a number of circumstances, including the then-futuristic use of IR array detectors on a 8-m class telescope. This has recently become reality: Richichi et al. (2006b) and Fors et al. (2006, 2008) reported

Send offprint requests to: A. Richichi

<sup>★</sup> Based on observations made with ESO telescopes at Paranal Observatory

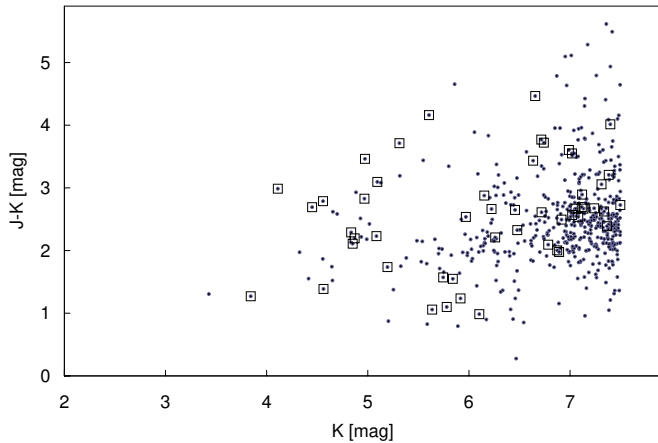


**Fig. 2.** Color-magnitude diagram for the sources of which we recorded LO events as listed in Table 1 (open squares). The small dots mark all sources occulted by the Moon in the same time span, to the limit  $K \leq 7.5$  mag.

in a preliminary form on the use of the ISAAC instrument in the so-called burst mode at the ESO VLT 8.2 m Antu telescope.

In the present paper we provide a detailed account of the observations carried out during a few hours in the night of March 21, 2006, when 51 LO events were recorded. A second batch of observations was carried out in August 2006: due to their large number and their different nature, these sources will be discussed in a separate paper. In Sect. 2 we describe the observations and we provide details of the data reduction. In Sect. 3 we discuss the results, which include new binaries, resolved stars and the near-IR counterparts of two radio maser sources. We also characterize the performance of this specialized observing mode, which combines the highest angular resolution and sensitivity possible today in the near-IR. In the conclusions we describe the integration of the LO technique in the service mode operations scheme in place at the Paranal observatory and our plans for routine LO observations at that site.

## 2. Observations and data analysis

We observed a passage of the Moon in a crowded region of the Galactic Bulge, in the night of March 21-22, 2006. The center of this region was located at  $\approx 17^{\text{h}}42^{\text{m}}$  and  $-28^{\circ}29'$ . Fig. 1 shows the area, with the apparent lunar path superimposed. It can be seen that, at closest approach, the limb of the Moon as seen from Paranal reached only a few arcseconds from the true Galactic Center. The region is heavily reddened by interstellar dust. A near-IR color-magnitude diagram is shown in Fig. 2. Due to extinction, few sources in this region of the sky have optical counterparts. Our LO predictions were based mostly on the 2MASS Catalogue (Cutri et al. 2003). To the limit  $K \leq 7.5$  mag a total of 509 sources were predicted to be occulted by the Moon in 5 hours. Our observations began at 6:11 UT and ended at 10:25 UT. A total of 51 events were recorded. The efficiency was limited in the first part of the observations by several missed or wrongly recorded events. In fact, this run represented a commissioning of the burst mode at ISAAC, which at the time had not yet been extensively tested. In the last part of the observations, with the technical aspects under control, the typical interval between recorded events was as short as three minutes and limited by the telescope pointing and data storing times.

The limit  $K \leq 7.5$  mag was quite arbitrary. In fact, in the same time span the number of occulted sources with  $K \leq 11$  mag was more than 15,000. As we will show later this magnitude limit would have been realistic, but it was clearly impossible to observe hundreds, not to mention thousands, of sources. Even a manual selection of the best ones would have been a daunting task, and for this we developed a prioritization rule which takes into account the magnitude, the color (redder objects were given more weight), and the time intervals between the events. We also flagged and gave additional priority to sources with previous observations or classification available in the SIMBAD database.

The lunar phase was -54%. In general LO observations are possible only on the dark lunar limb, thus we observed reappearances: the telescope was pointed at the nominal star position while this was still occulted, and data were recorded starting about thirty seconds before the nominal reappearance time. In reality, predictions resulted accurate to few seconds in all cases. Thanks to the work of Paranal software engineers, the event times were included in the files that control telescope and instrument operation (so-called Observing Blocks or OBs). These latter were then loaded well in advance, and data acquisition would start automatically at the preset time.

Two factors affected significantly the quality of the resulting data. Firstly, the active optics corrections of the primary mirror had to be switched off. As a result, the image quality was rather poor especially in the first part of the run. Towards the end of the run, we activated the active optics a few times in-between events, thus obtaining much better image quality. Secondly, in a few cases part of the signal fell outside the sub-window (clipping). Blind pointing was done by means of offsets from a nearby star but, given also the bad image quality and the small detector sub-window, it was sometimes not sufficiently accurate. The sub-window was kept to  $64 \times 64$  pixels, or  $\approx 9.5''$  squared, in order to achieve sufficiently fast read-outs. We stress that in general this does not have too many negative effects on the occultation light curve except of course for the signal-to-noise ratio (SNR). Fig. 3 illustrates the above mentioned effects.

The critical parameter for the angular resolution achieved in a LO, along with the signal-to-noise ratio (SNR), is the sampling of the light curve. For this, the burst mode implemented on the Aladdin detector of the ISAAC instrument was the critical factor, allowing us to obtain times of just 3.2 ms on a  $32 \times 32$  subarray and 6.4 ms sampling on a  $64 \times 64$  subarray. In order to increase the accuracy of source centering during blind pointing of the occulted sources, all the events but the first two were recorded in  $64 \times 64$  mode. The length of the data stream was kept between 8000 and 14000 frames (see Table 1). We do not describe here the details of the burst mode for ISAAC, for which we refer to Richichi et al. (2008). The burst mode is also possible at several other ESO instruments both at Paranal and La Silla (see for example Domiciano de Souza et al. 2008, Poncelet et al. 2007, Sicardy et al. 2007). The raw data need to be reformatted in proper FITS files, which are then processed using the AWLORP pipeline. Schematically, this latter performs both an automated light curve extraction based on a mask estimation which preserves the object-pixel connectivity, and computes an automated estimation of the basic parameters of each light curve, namely time of occultation, stellar signal, background signal, and rate of lunar motion. This is achieved via a novel algorithm based on wavelet-decomposition. Details on AWLORP can be found in Fors (2006) and Fors et al. (2008).

Once the data are prepared with the proper structure, AWLORP runs automatically, saving the user from a lengthy and error-prone screening and producing preliminary fits and plots

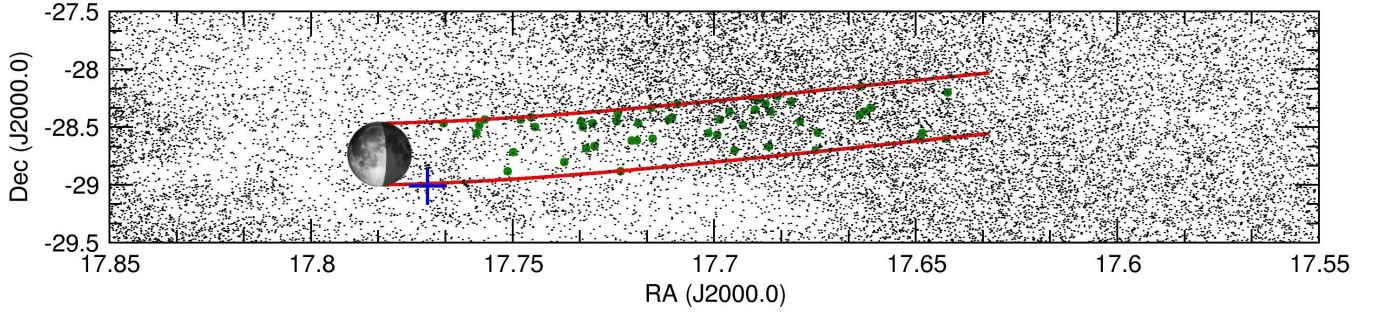


**Fig. 1.** The area close to the sources occulted by the Moon in the night of March 21, 2006. The small dots represent sources in the 2MASS catalogue with magnitude  $K \leq 7.5$ . The heavier dots are the sources for which we could record a lunar occultation. The apparent path of the Moon, moving from West to East, is also shown. The cross marks the Galactic Center.

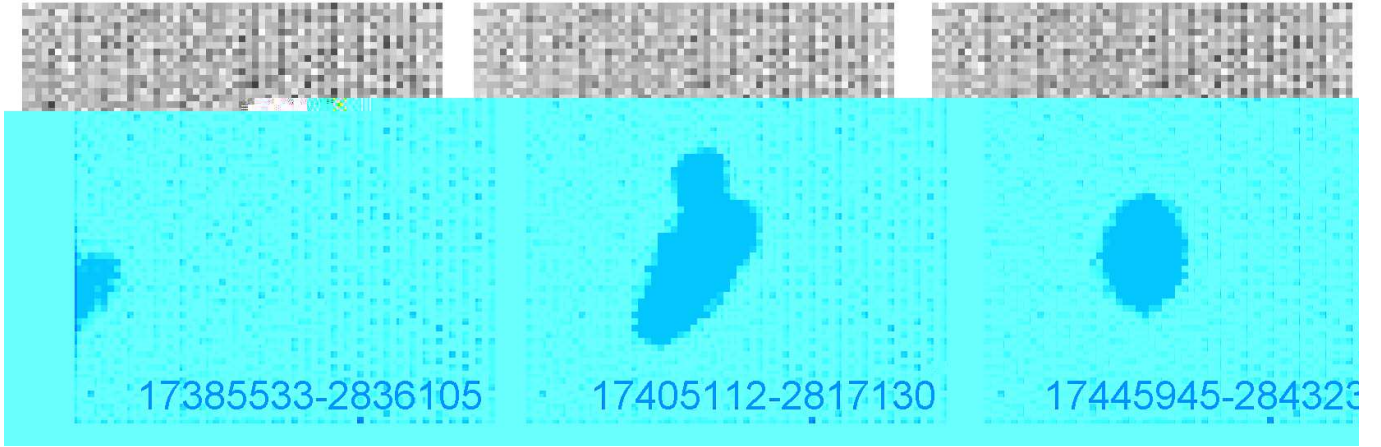


**Fig. 3.** Illustration of the adverse effects of image clipping due to inaccurate blind pointing (left) and of poor image quality due to the active optics being switched off (middle, note that the target is a single star), as described in the text. The right figure is an example of a more regular case, for comparison. All three figures are time averages over several thousand frames on the subwindow of the Aladdin array in ISAAC. The windows are  $\approx 9.5''$  on the side. The 2MASS names of the occulted stars are indicated.

for all light curves. A total of 30 events were found to have data of sufficient quality: the remaining 21 were discarded because of problems in the pointing or in the data acquisition. For the data analysis, we employed the model-dependent fitting ALOR (see Richichi et al. 1996) and the model-independent estimation of the brightness profile CAL (Richichi 1989).

### 3. Results

The complete list of recorded occultation events is given in Table 1. It includes comments about the quality of the data and missed events. The K-band magnitudes range from 4.1 to 7.4. In the table, and throughout the paper, we use 2MASS names. Most of the sources do not have a counterpart in the Simbad database. Only 14 of the sources reliably recorded can be cross-identified with optical or IR sources, and these are also listed in the table.

We have tested the resolved/unresolved character of all the sources, using the method first outlined by Richichi et al. (1996) and applied in some of our previous papers such as in Fors et al. (2004) and Richichi et al. (2006a). The results are shown in Fig. 4, and we discuss below separately the resolved and the unresolved sources.

We show in the following just two examples of recorded light curves along with their best fits. The complete set of light curves and fits is available online. In spite of the previously mentioned problems, we note that our sample includes some of the best LO

data ever recorded, both in terms of sensitivity and of SNR. The performance of the 8.2 m VLT telescope for LO work proved to be outstanding, not just due to its light collecting power but also to the great reduction of atmospheric scintillation - which is often the main limiting SNR factor for LO. In terms of angular resolution, the relationship shown in Fig. 4 is consistent with that established at other, smaller telescopes for which the detector integration time (DIT) was considerably shorter (see Richichi et al. 1996, 2006a). We note that the SNR of the fit shown in Fig. 5 is, as far as we know, the best ever achieved for a LO light curve. Just a few milliarcseconds away from the main star it would have been possible to detect a companion fainter than the primary by 7.8 and 7.1 mag in the occulted and unocculted part respectively, i.e. on opposite sides of the star. This compares favorably with the best AO-assisted high-contrast imaging close to a bright star on this range of separations (Masciadri et al. 2005).

#### 3.1. Resolved sources

We have found two sub-arcsecond (projected) separation binaries, two stars with a convincingly resolved angular size, and three other stars which we consider as marginally resolved. These sources are listed in Table 2, using the same format already used in Richichi et al. (2006a) and other papers in that series. In summary, the columns list the absolute value of the fitted linear rate of the event  $V$ , its deviation from the predicted

**Table 1.** List of the recorded occultation events

2MASS id	Frame (px)	NDIT	Time (UT)	K (mag)	J-K	Sp	Cross-Id	Notes
17383314-2836158	32	14000	06:11:57	5.64	1.06	—	—	df, 50% off edge
17383141-2812445	32	14000	06:15:19	6.78	2.09	—	—	df
17394834-2809136	64	12000	06:23:51	6.48	2.33	—	—	near terminator
17385533-2836105	64	12000	06:28:10	7.34	2.62	—	—	df, 50% off edge
17385407-2833227	64	12000	06:32:56	7.13	2.67	—	—	df, 50% off edge
17391567-2826194	64	12000	06:47:58	6.46	2.65	—	—	df
17394022-2820124	64	12000	06:55:09	7.12	2.69	—	—	df, close to edge
17394602-2822089	64	12000	07:00:05	7.05	2.67	—	—	df
17395038-2824061	64	12000	07:04:00	5.78	1.10	—	CD-28 13409	not seen
17410318-2814151	64	12000	07:08:12	7.02	2.57	—	—	edge (75% off)
17402920-2842361	64	12000	07:14:29	7.50	2.73	—	—	not seen
17405112-2817130	64	12000	07:18:35	4.87	2.20	M6.5	[RHI84] 10-333	df
17412116-2816010	64	12000	07:22:54	5.84	1.55	M5	[RHI84] 10-356	df, 2 stars
17402750-2833099	64	12000	07:26:35	7.24	2.67	—	—	not seen
17411415-2818051	64	12000	07:29:49	6.87	2.00	M5	[RHI84] 10-352	df, 2 stars
17404347-2827185	64	12000	07:33:08	6.89	1.98	—	—	df, 50% off edge
17410937-2822418	64	12000	07:39:35	6.92	2.49	—	DENIS-P J174109.4-282242	df
17412349-2821538	64	12000	07:44:18	7.37	2.39	—	—	df
17411109-2840486	64	12000	07:47:31	7.31	3.06	—	—	not seen
17423294-2818473	64	12000	07:52:21	3.84	1.27	G8Iab	HD 160706	near terminator
17414641-2822593	64	12000	07:57:10	5.09	2.23	—	ISOGAL-P J174146.5-282301	df
17413435-2829225	64	12000	08:01:38	4.85	2.11	—	DENIS-P J174134.4-282922	df, 10% off edge
17414185-2842287	64	12000	08:05:22	6.22	2.66	—	—	not seen
17415470-2826596	64	12000	08:09:09	7.08	2.54	—	DENIS-P J174154.7-282659	df, 95% off edge
17425620-2820370	64	12000	08:13:32	4.56	1.39	—	2MASS J17425620-2820370	not seen
17415719-2834236	64	12000	08:17:55	7.12	2.89	—	—	very faint
17420509-2833465	64	12000	08:22:10	6.15	2.88	—	—	df, 50% off edge
17423746-2825311	64	12000	08:27:23	5.20	1.74	—	—	df, very faint
17424039-2826255	64	12000	08:31:04	4.56	2.79	—	IRAS 17395-2825	not seen
17432345-2853503	64	12000	08:38:21	4.97	3.46	—	ISOGAL-P J174323.6-285349	not seen
17432585-2823598	64	12000	08:44:05	5.92	1.24	—	—	df, 15% off edge
17430791-2828016	64	12000	08:48:53	7.02	3.55	—	—	df
17425497-2836593	64	12000	08:53:18	6.72	3.77	—	—	df, 50% off edge
17432661-2827590	64	12000	08:58:32	6.26	2.21	M2:	[RHI84] 10-443	df, 50% off edge
17430901-2837039	64	12000	09:01:53	6.99	3.60	—	—	df, 30% off edge
17431348-2837004	64	12000	09:04:34	6.74	3.72	—	—	df
17434830-2828129	64	12000	09:10:32	4.84	2.29	—	—	df, 95% off edge
17435893-2827521	64	12000	09:15:00	5.97	2.54	—	—	df, second star
17444369-2825027	64	12000	09:17:24	7.38	3.21	—	—	df, 5% off edge
17435704-2830432	64	12000	09:21:47	5.61	4.16	—	IRAS 17407-2829	df, 25% off edge
17434681-2840176	64	12000	09:26:43	4.45	2.69	M6.5	ISOGAL-P J174346.6-284017	not seen
17435399-2841285	64	12000	09:31:28	4.11	2.99	—	IRAS 17407-2840	df
17445251-2826479	64	12000	09:36:45	5.09	3.10	—	—	not seen
17441366-2848501	64	8000	09:39:53	6.10	0.99	K0	HD 316221	5% off edge
17443976-2830568	64	10000	09:46:46	7.40	4.01	—	—	not seen
17452448-2826434	64	12000	09:49:33	6.72	2.61	—	—	not seen
17450413-2853412	64	12000	10:05:20	5.75	1.57	M2	[RHI84] 10-515	df
17452968-2829325	64	12000	10:10:43	6.64	3.43	—	—	gf, 2 more stars
17445945-2843238	64	12000	10:14:15	4.97	2.83	—	—	gf
17460150-2828035	64	12000	10:19:24	6.66	4.47	—	—	gf
17453224-2833429	64	12000	10:25:26	5.31	3.71	—	ISOGAL-P J174532.3-283338	gf, 5% off edge

Frame is the size of the subwindow and NDIT the number of frames used in the raw burst mode. The number of frames in the reformatted FITS cube is NDIT/2-1, and this also determines the total time span of the recorded data. In the notes, df stands for defocused and gf for good focus.

**Table 2.** Summary of results.

(1) Source	(2)  V  (m/ms)	(3) V/V <sub>t</sub> -1	(4) $\psi(^{\circ})$	(5) PA( $^{\circ}$ )	(6) CA( $^{\circ}$ )	(7) SNR	(8) Sep. (mas)	(9) Br. Ratio	(10) $\phi_{UD}$ (mas)
17391567-2826194	0.7702	-2.9%	-7	268	163	211.0			2.68 $\pm$ 0.66
17412116-2816010	0.3245	5.7%	-2	350	245	105.4	711.7 $\pm$ 3.4	22.6 $\pm$ 0.8	
17435893-2827521	0.4688	4.9%	-3	321	222	233.2			2.22 $\pm$ 0.37
17444369-2825027	0.1802	62.3%		see text		68.2	171.6 $\pm$ 25.8	47.8 $\pm$ 7.5	
17435399-2841285	0.6095	-1.4%	-5	266	168	460.0			2.36 $\pm$ 0.11
17445945-2843238	0.5945	-1.7%	-7	263	168	251.4			1.91 $\pm$ 0.30
17453224-2833429	0.5328	7%	-6	302	209	126.9			2.9 (shell)



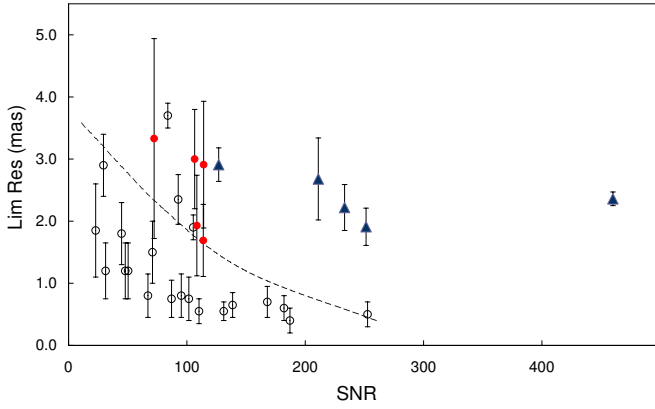


**Fig. 4.** Sources for which an upper limit on the angular diameter could be established using the method described in the text are marked with outlined circles. The filled circles are sources for which an angular diameter could be formally established, but for which the associated errorbar is such that they are undistinguishable from being unresolved. The dashed line is an arbitrary representation of a tentative SNR-limiting angular resolution relationship. The triangles are sources for which the angular diameter and associated error lies tentatively or convincingly above the limiting angular resolution.

rate  $V_l$ , the local lunar limb slope  $\psi$ , the position and contact angles, the signal-to-noise ratio (SNR). For binary detections, the projected separation and the brightness ratio are given, while for resolved stars the angular diameter  $\phi_{UD}$  is reported, under the assumption of a uniform stellar disc. All angular quantities are computed from the fitted rate of the event.

Several of our acquisition images show companions, but we report only two binaries which have projected separations below one arcsecond. This is rather large for the context of LO binary detections. In fact, for separations  $\geq 0''.5$  the LO technique is relatively inaccurate, due to possible differences in the local limb slope at the points of occultation of the two components. The two objects are 2MASS 17412116-2816010 and 2MASS 17444369-2825027. They are most likely projection and not physical pairs: we report them here for completeness, since no previous mention was present in the literature. The former was classified by Raharto et al. (1984) as a M5 star. We note that the difference between predicted and observed lunar rate for the second star was quite significant, as reported in Table 2. The contact angle for this event was only  $260^\circ$ , i.e. nearly grazing, and the predicted lunar rate only  $-0''.1/s$ . Under these conditions, it is not uncommon that either a small error in the predictions or a local limb slope can significantly alter the computation of the effective PA and CA.

The remaining stars in Table 2 are those which appear significantly different from point-like. The two most interesting ones are 2MASS 17435399-2841285 and 2MASS 17453224-2833429, which happen to be both masing AGB stars. Unfortunately the distance determination for these stars is uncertain, especially in the absence of detailed photometric and pulsational properties. The former has an angular size which, albeit small in absolute terms, appears to be convincingly established (see Fig. 4 and Fig. 5). This star is cross-identified with IRAS 17407-2840, a SiO maser previously measured by Messineo et al. (2002, 2004, 2005). Its radial velocity is negative and cannot be used for a kinematic distance, but Messineo (priv. comm.) estimates a distance of 3.7 kpc based on the average extinction

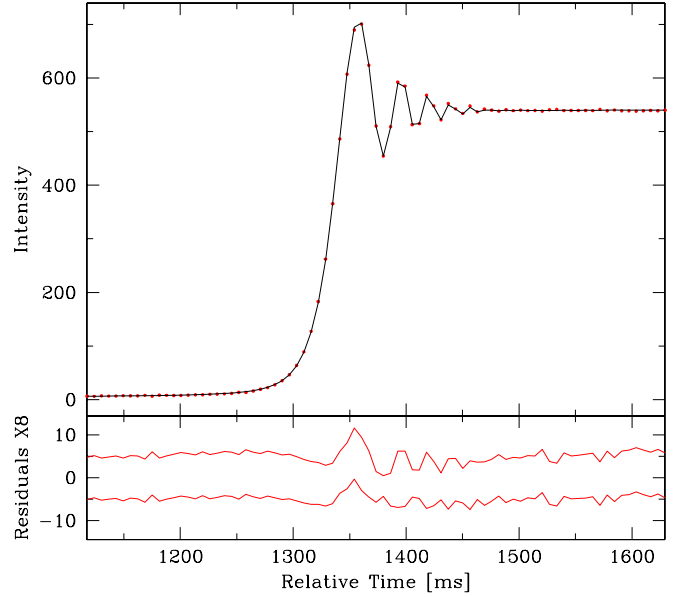


**Fig. 5.** *Top:* data (dots) and best fit (solid line) for 2MASS 17435399-2841285. *Bottom:* enlarged by eight and displaced by arbitrary offsets for clarity, the residuals of the fits with a point-like source (above,  $\chi^2 = 2.0$ ) and with a uniform-disk model, resulting in a diameter of  $2.36 \pm 0.11$  mas (below,  $\chi^2 = 1.1$ ).

and the model of Drimmel (2003). According to this, the angular size listed in Table 2 would translate to over 8 AU. Apart from consideration on the distance uncertainty, it is likely that the LO-derived size is not indicative of an uniform-disk diameter but rather a mix of the photosphere and the immediate circumstellar emission.

2MASS 17453224-2833429 has a similar nature and set of references, with the addition of Sjouwerman et al. (2004). The fit for this source gave a SNR of 127 which is lower than expected for the magnitude of this source ( $K=5.1$  mag), and the UD size reported in Table 2 should be considered only as an indication. A model-independent analysis by CAL revealed a faint but well defined extended emission around the central component, as shown in Fig. 6. The profile of this emission is almost symmetrical, has the rim brightening typical of optically thin shells and is consistent with the masing nature of this star. In this case both a kinematic and an extinction distance can be estimated, at 4.5 and 3.3 kpc respectively (Messineo, priv. comm.). By using their average, the inner shell radius of 10-15 mas would translate to  $\approx 40$  AU. We note that the residuals of the uniform-disk model for 2MASS 17435399-2841285 indicate the possibility of a circumstellar shell being detected also in this case (cfr. Fig. 5), but given that the  $\chi^2$  was already significantly good we did not proceed with more extreme fits. The different signatures of the shell for these two maser stars could be related to their difference in J-K color (3.0 versus 3.7 mag).

The remaining three stars in Table 2 appear resolved, although their location above the SNR-resolution relationship of Fig. 4 is less definite than for the two maser stars just mentioned and we prefer to consider their diameters as tentative for the moment. There are no known cross-identifications or literature entries for these stars.

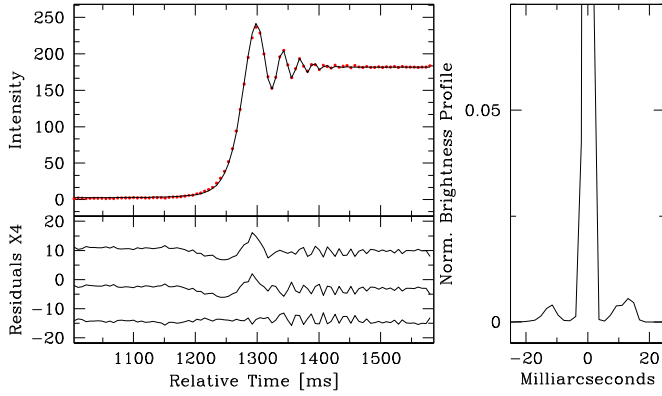


**Fig. 6.** *Left:* upper panel, data (dots) and best fit (solid line) for 2MASS 17453224-2833429. The lower panel shows, on a scale enlarged by four and displaced by arbitrary offsets for clarity, the residuals of three different fits. Top, fit with a point-like source ( $\chi^2 = 7.0$ ). Middle, fit with a uniform-disk model, resulting in a diameter of  $2.91 \pm 0.27$  mas ( $\chi^2 = 6.3$ ). Bottom, fit with the model-independent CAL method ( $\chi^2 = 1.6$ ), by far the most convincing. *Right:* brightness profile reconstructed by the CAL method, corresponding to the residuals of the lowermost fit on the left.

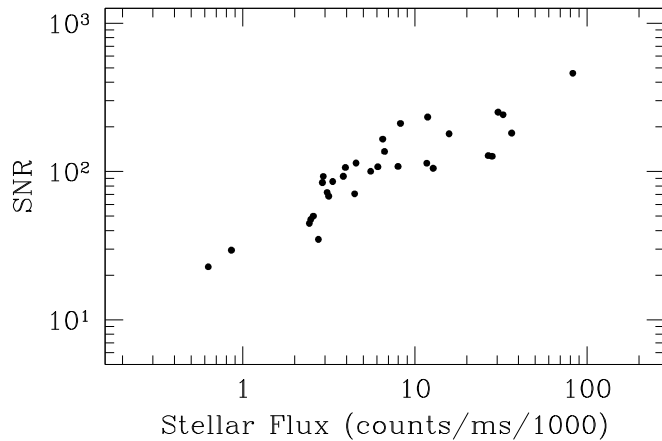


**Fig. 7.** Plot of the SNR achieved in our fits of both resolved and unresolved source, as a function of the total measured flux.

### 3.2. Unresolved stars and performance

Most of the stars in our sample appear unresolved, as is to be expected from random observations of field stars. Richichi et al. (2006a) have discussed the incidence of binary stars in such samples for LO observations based on the 2MASS catalogue, and our present results are consistent within the uncertainty of small statistics. The unresolved stars are also useful, namely in that the relationship of Fig. 4 establishes rather strict upper limits on their size and on the brightness ratio of unseen components, if any. Thus these stars can be safely used as calibrators for long-baseline interferometry.

Further, the unresolved stars allow us to investigate the performance of the burst mode at the VLT for LO, similar to what was done for other instrument and telescope configurations in the past (see Fors et al. 2004). In Fig. 7 we plot the SNR achieved in the fits of all sources (the unresolved ones being the majority), against the total measured flux. This is a better quantity to use than the actual magnitude, since as mentioned earlier many of our sources were recorded at the edge of the subarray field with

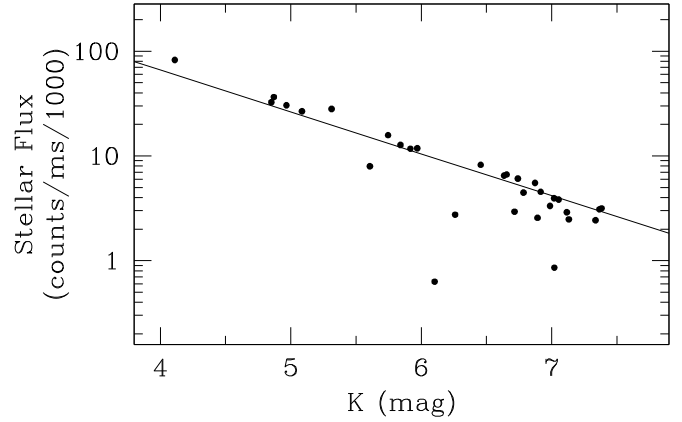


**Fig. 8.** Plot of the total measured flux against the K magnitude of the sources (from 2MASS). The line shows the expected counts, based on the ISAAC Exposure Time Calculator. Note the discrepant cases, due to the problems mentioned in the text.

considerable loss of signal. Also intrinsic variability might be a cause for some of the stars. Indeed, Fig. 8 shows many outliers from the ideal K magnitude-observed flux are present. Using the measured signal instead, Fig. 7 shows a rather linear relationship across over two orders of magnitudes in flux. This implies that at the faint end we were still in a photon-limited regime, and at the bright end the incidence of scintillation and possible non-linearities was not yet significant. We estimate that non-linearity of the detector should become important above  $K \approx 3$  mag, i.e. one magnitude above our brightest target for this run.

In spite of the outliers, the relationship between K magnitude and counts clearly emerges from Fig. 8, and it is in excellent agreement with the expected ISAAC performance. Comparing the two figures, we estimate at first approximation that under the same conditions of sampling and DIT (6.4 ms) it should have been possible to obtain  $\text{SNR}=1$  for  $K \approx 12$  mag. This is the minimum SNR necessary to detect a faint companion in a LO light curve, although measurements of angular diameters or extended emission would require  $\text{SNR} \geq 10$ . We note that, at the faint magnitude end, critical parameters are the diffuse scattered light background, which is a function of the lunar phase and distance of the occultation point from the terminator, and the pixel scale. Ideally, this latter should match the seeing disc, but in our case with a pixel scale of about  $0''.148$  we significantly oversampled the background.

## 4. Conclusions

We have presented the first LO results obtained using the so-called burst mode of the ISAAC instrument at the ESO Antu VLT telescope. This mode permits to record data streams on a small subarray at high temporal frequency (3.2 ms, although mostly 6.4 ms were used for the present work). We recorded 51 occultation events over about four hours during a close approach of the Moon to the Galactic Center. The events were reappearances from behind the dark limb. This, coupled with initial problems of focussing and image quality due mostly to the commissioning nature of the run, resulted in several sources being missed or without sufficient quality. Nevertheless, 30 of the events resulted in light curves of good, or even excellent quality, including some of the best SNR traces ever recorded with this technique. We have revealed two binaries, three stars with a marginally resolved angular diameter of the order of

2 mas, and two resolved masing AGB stars which appear to be in the foreground of the galactic bulge. For one of these, 2MASS 17453224-2833429, we were able to recover the brightness profile of the extended emission. This has the typical signature of an optically thin shell, with inner radius of order 10-15 mas, corresponding to about 40 AU. Follow-up studies are required to obtain further information on these stars, given that they are all heavily reddened and most have no known counterpart or literature entries.

Our analysis, including the unresolved sources, has established an unprecedented performance of the LO technique in the near-IR using a very large telescope and a fast read-out mode. We find that the angular resolution varies between 4 and 1 mas, and even less in the case of very high SNR. Data quality is generally impressive, compared to smaller telescopes, mostly due to the scintillation reduction effect of the large mirror. The dynamic range is also significantly improved with respect to previous observations, and we have shown that in some cases it would have been possible to detect a companion fainter than the primary by about 8 magnitudes in broad K band on angular scales comparable to the Airy disk of the telescope. This result compares favorably with other AO-assisted high contrast imaging techniques.

The random selection of sources to be occulted and the fixed-time nature of the events remain the main downsides of the LO technique. However, thanks to the very short telescope time required for each observation, LO are an ideal filler program for times when the telescope is idle or other programs cannot be conveniently executed. The service mode observations implemented at the VLT provide the right context for this, and we have obtained approval for such a filler program during ESO observing periods 80 and 81 (from October 2007 through September 2008). Several hundreds of OBs have been prepared for each period, and are in the queue awaiting execution whenever five minutes of telescope time become available.

*Acknowledgements.* This work is partially supported by the *ESO Director General's Discretionary Fund* and by the *MCYT-SEPCYT Plan Nacional I+D+I AYA #2005-08604*. AR wishes to thank the National Astronomical Observatory of Japan in Mitaka, and Dr. J. Nishikawa in particular, for their hospitality during a prolonged stay which led to the final writing of this paper. We thank Dr. M. Messineo for private communications on the properties of the SiO masers reported in this paper. This research has made use of the SIMBAD database, operated at CDS, Strasbourg, France.

## References

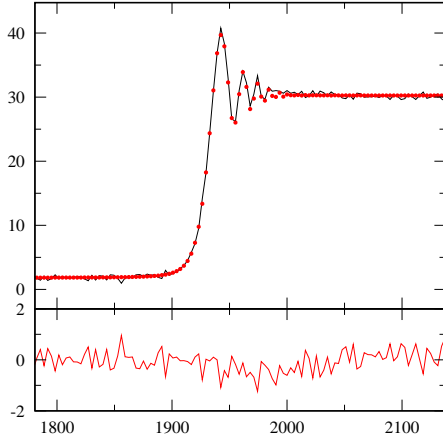
- Cutri, R. M., Skrutskie, M. F., van Dyk, S. et al. 2003, The IRSA 2MASS All-Sky Point Source Catalog, NASA/IPAC Infrared Science Archive
- Domiciano de Souza, A., Kervella, P., Bendjoya, P., & Niccolini, G. 2008, A&A, 480, L29
- Drimmel, R., Cabrera-Lavers, A., López-Corredoira, M. 2003, A&A, 409, 205
- Fors, O. 2006, Ph.D. Thesis, Departament d'Astronomia i Meteorologia, Universitat de Barcelona
- Fors, O., Richichi, A., Núñez, J., Prades, A. 2004, A&A, 419, 285
- Fors O., Richichi, A., Mason, E., Stegmeier, J., Chandrasekhar, T. 2006, Highlights of Spanish Astrophysics IV, Figueras et al. (Eds.), Springer 2007
- Fors, O., Richichi, A., Otazu, X., & Nuñez, J. 2008, A&A, 480, 297
- Masciadri, E., Mundt, R., Henning, T., Alvarez, C., & Barrado y Navascués, D. 2005, ApJ, 625, 1004
- Messineo, M., Habing, H. J., Sjouwerman, L. O., Omont, A., & Menten, K. M. 2002, A&A, 393, 115
- Messineo, M., Habing, H. J., Menten, K. M., Omont, A., & Sjouwerman, L. O. 2004, A&A, 418, 103
- Messineo, M., Habing, H. J., Menten, K. M., Omont, A., Sjouwerman, L. O., & Bertoldi, F. 2005, A&A, 435, 575
- Poncet, A., Doucet, C., Perrin, G., Sol, H., & Lagage, P. O. 2007, A&A, 472, 823
- Raharto, M., Hamajima, K., Ichikawa, T., Ishida, K., Hidayat, B. 1984, Ann. Tokyo Astron. Obs., 19, 469
- Richichi, A. 1985, Thesis, Faculty of Physics, Florence University (in italian)

- Richichi, A. 1989, A&A, 226, 366
- Richichi, A. 1997, IAU Symp. 158: Very High Angular Resolution Imaging, 158, 71
- Richichi, A., Baffa, C., Calamai, G., Lisi, F. 1996, AJ, 112, 2786
- Richichi, A., Percheron, I., Khristoforova, M. 2005, A&A, 431, 773
- Richichi, A., Fors, O., Merino, M. et al. 2006a, A&A, 445, 1081
- Richichi, A., Fors, O., Mason, E., Stegmeier, J. 2006b, The Messenger, 126, 24
- Richichi, A., Fors, O., Mason, E., Stegmeier, J. , Proc. of the ESO Workshop Science with the VLT in the ELT Era, A. Moorwood (ed.), in press
- Sicardy, B., et al. 2007, AAS/Division for Planetary Sciences Meeting Abstracts, 39, #62.02
- Sjouwerman, L. O., Messineo, M., & Habing, H. J. 2004, PASJ, 56, 45

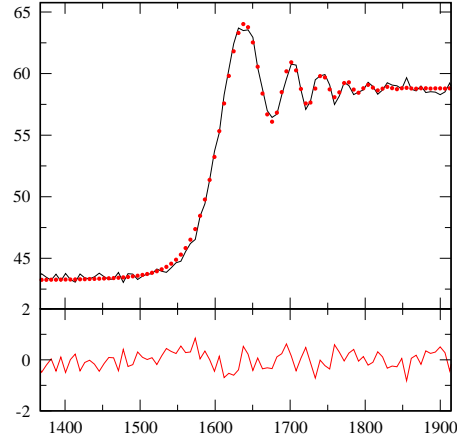
# Online Material



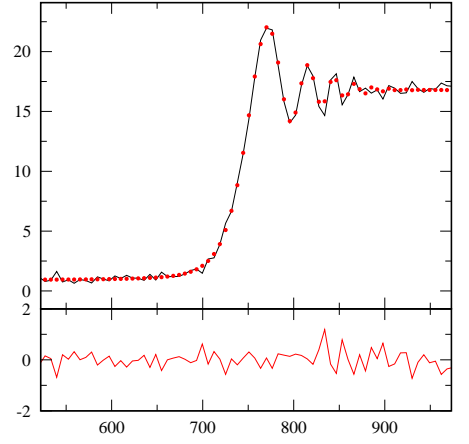
17383141-2812445



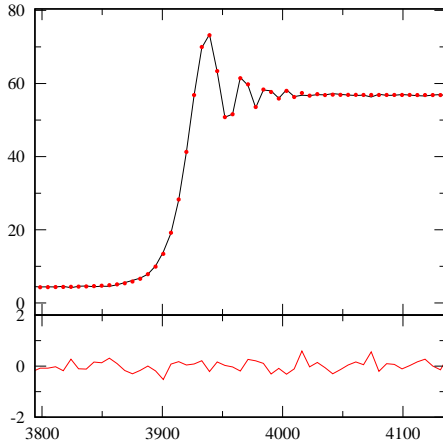
17385533-2836105



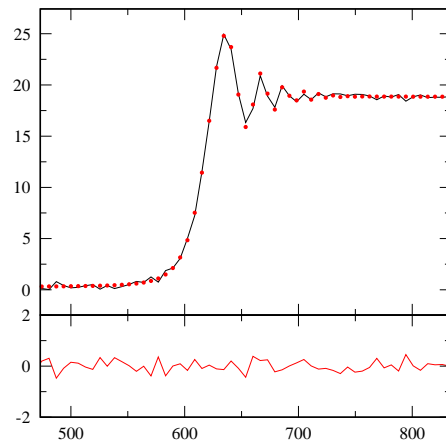
17385407-2833227



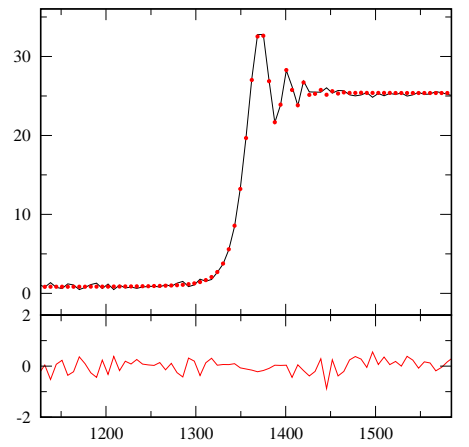
17391567-2826194



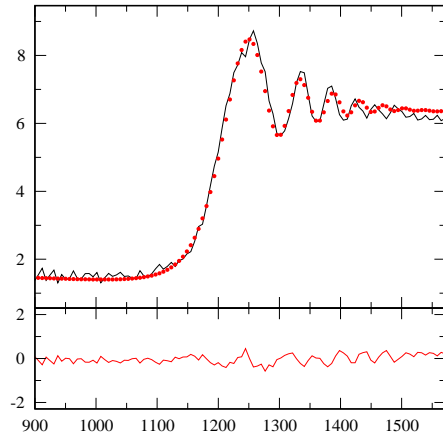
17394022-2820124



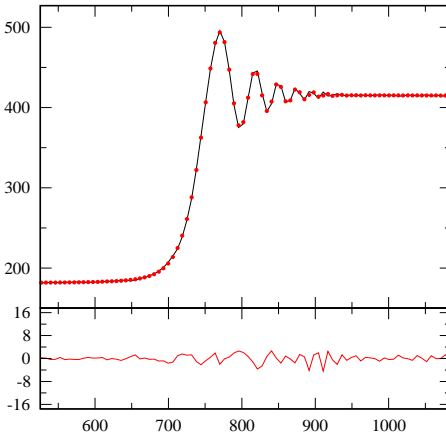
17394602-2822089



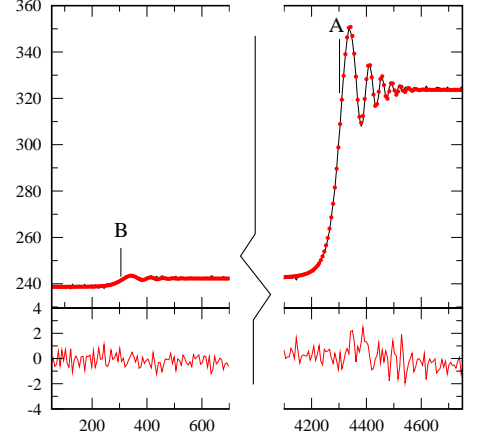
17410318-2814151



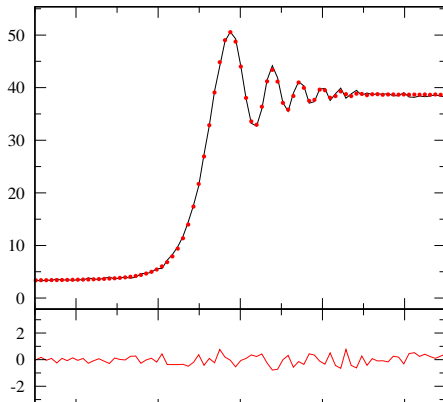
17405112-2817130



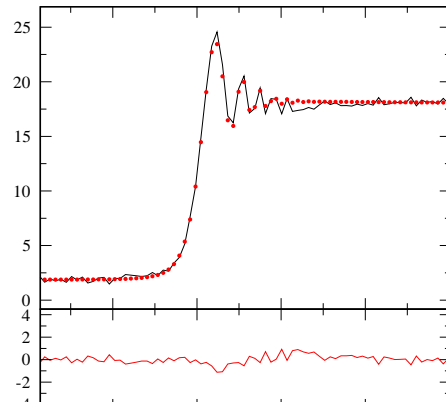
17412116-2816010



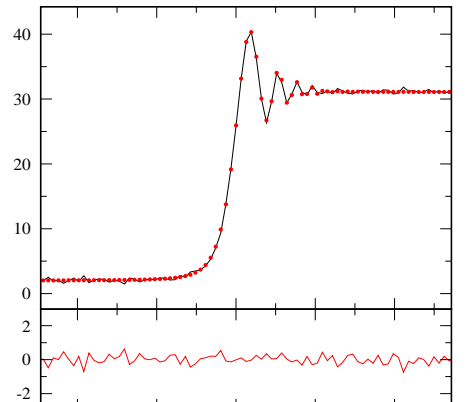
17411415-2818051

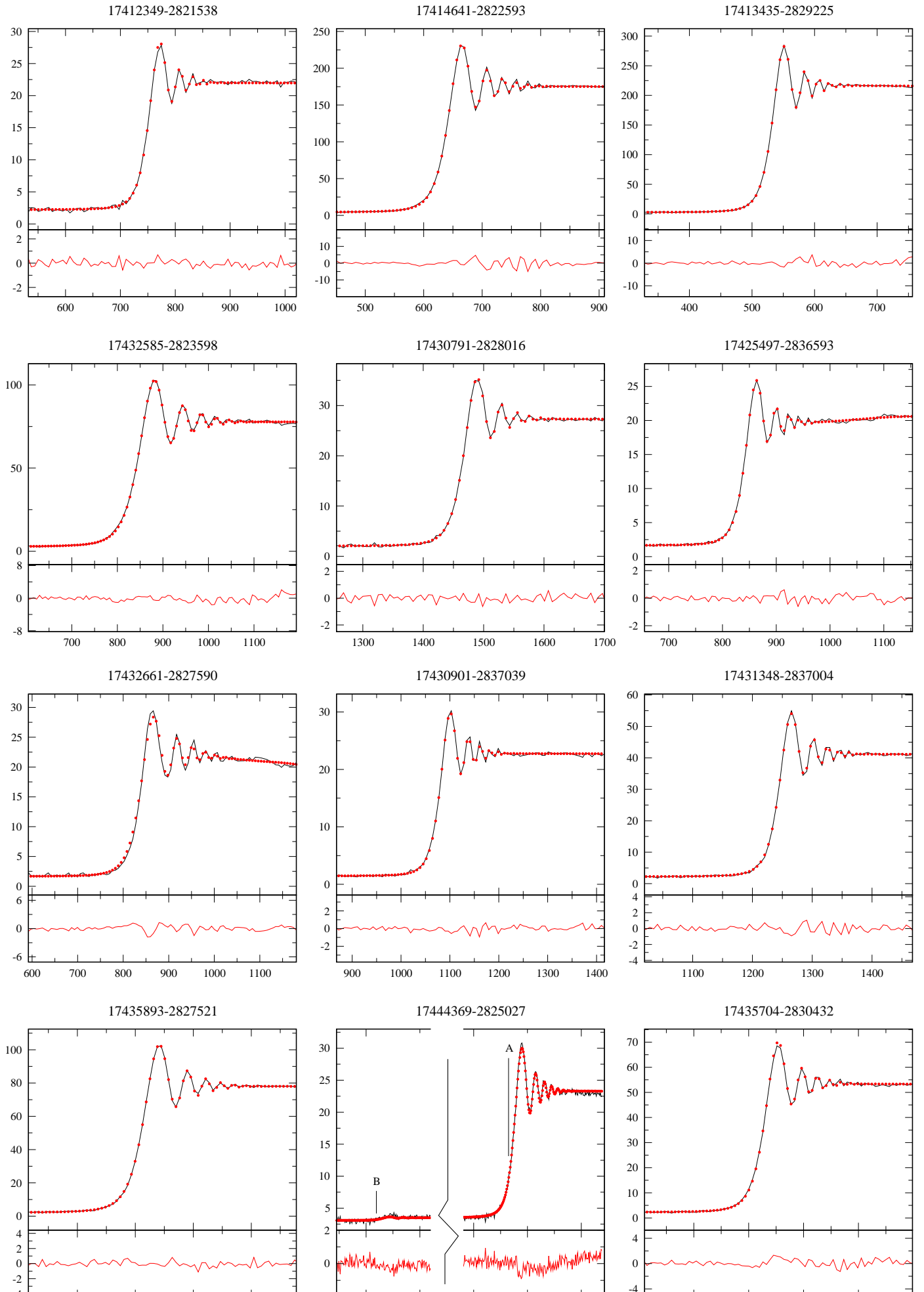


17404347-2827185

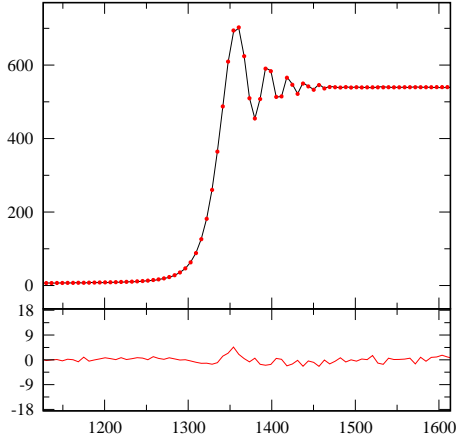


17410937-2822418

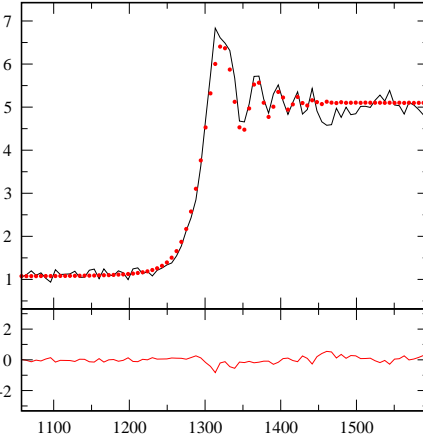




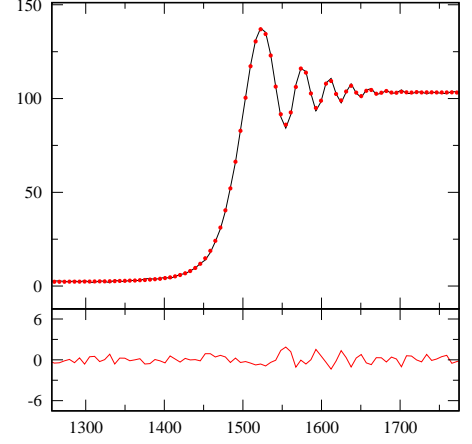
17435399-2841285



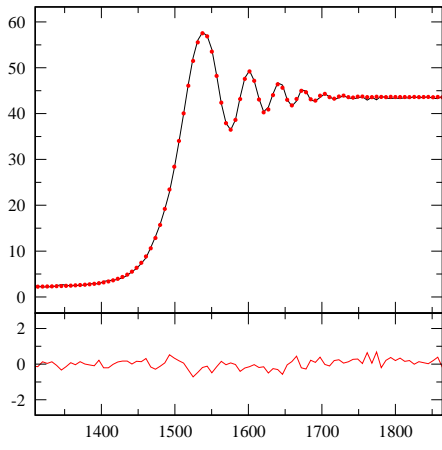
17441366-2848501



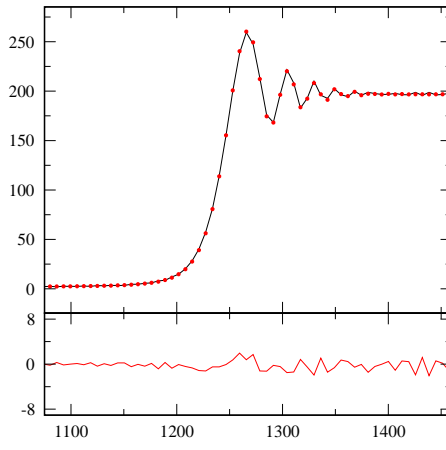
17450413-2853412



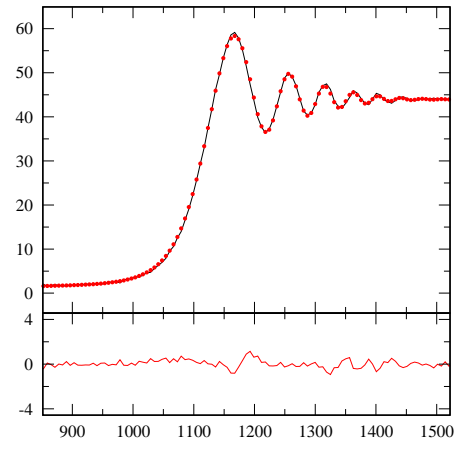
17452968-2829325



17445945-2843238



17460150-2828035



17453224-2833429

